



Research article

HDAC6 inhibitor ACY-1215 protects from nonalcoholic fatty liver disease via inhibiting CD14/TLR4/MyD88/MAPK/NFκB signal pathway

Shifeng Fu^{a,b,c}, Mengmeng Xu^{a,b,c}, Jianglei Li^{a,b,c}, Meihong Yu^{a,b,c},
Siyi Wang^{a,b,c}, Liu Han^{a,b,c}, Rong Li^{a,b,c}, Feihong Deng^{a,b,c}, Hailing Peng^{a,b,c,d},
Deliang Liu^{a,b,c,**}, Yuyong Tan^{a,b,c,*}

^a Department of Gastroenterology, Second Xiangya Hospital, Central South University, Changsha, 410011, Hunan Province, China

^b Research Center of Digestive Diseases, Central South University, Changsha, 410011, Hunan Province, China

^c Clinical Research Center of Digestive Diseases of Hunan Province, Changsha, 410011, Hunan Province, China

^d Longshan County People's Hospital, Longshan, 416899, Hunan Province, China

ARTICLE INFO

Keywords:

Nonalcoholic fatty liver disease
Histone deacetylation 6
ACY-1215
CD14
TLR4

ABSTRACT

Background & aims: Nonalcoholic fatty liver disease (NAFLD) is a chronic liver disease characterized by hepatic steatosis, for which there is currently no effective treatment. ACY-1215 is a selective inhibitor of histone deacetylation 6, which has shown therapeutic potential in many tumors, as well as acute liver injury. However, no research about ACY-1215 on NAFLD has been published. Therefore, our study aims to explore the role and mechanism of ACY-1215 in the experimental model of NAFLD, to propose a new treatment strategy for NAFLD.

Methods: We established cell and animal models of NAFLD and verified the effect of ACY-1215 on NAFLD. The mechanism of ACY-1215 on NAFLD was preliminarily explored through TMT relative quantitative proteomics, and then we verify the mechanism discovered in the experimental model of NAFLD.

Results: ACY-1215 can reduce lipid aggregation, IL-1β, and TNF α mRNA levels in liver cells in vitro. ACY-1215 can reduce the weight gain and steatosis in the liver of the NAFLD mouse model, alleviate the deterioration of liver function, and reduce IL-1βs and TNF α mRNA levels in hepatocytes. TMT relative quantitative proteomics found that ACY-1215 decreased the expression of CD14 in hepatocytes. It was found that ACY-1215 can inhibit the activation level of CD14/TLR4/MyD88/MAPK/NFκB pathway in the NAFLD experimental model.

Conclusions: ACY-1215 has a protective effect on the cellular model of NAFLD induced by fatty acids and lipopolysaccharide, as well as the C57BL/6J mouse model induced by a high-fat diet. ACY-1215 may play a protective role by inhibiting CD14/TLR4/MyD88/MAPK/NFκB signal pathway.

* Corresponding author. No.139 Renmin Road, Furong district, Changsha city, Hunan province, China.

** Corresponding author. No.139 Renmin Road, Furong district, Changsha city, Hunan province, China.

E-mail addresses: deliangliu@csu.edu.cn (D. Liu), tanyuyong@csu.edu.cn (Y. Tan).

<https://doi.org/10.1016/j.heliyon.2024.e33740>

Received 4 March 2024; Received in revised form 19 June 2024; Accepted 26 June 2024

Available online 27 June 2024

2405-8440/© 2024 The Authors. Published by Elsevier Ltd. This is an open access article under the CC BY-NC license (<http://creativecommons.org/licenses/by-nc/4.0/>).

Abbreviations

Abbreviation	Full name
NAFLD	nonalcoholic fatty liver disease
NAFL	nonalcoholic fatty liver
NASH	nonalcoholic steatohepatitis
HCC	hepatocellular carcinoma
ALT	alanine aminotransferase
AST	aspartate aminotransferase
TG	triglyceride
T2DM	type 2 diabetes
DNA	deoxyribonucleic acid
HDAC	histone deacetylase
HDACi	histone deacetylase inhibitor
HFD	high fat diet
TLR4	toll-like receptor 4
MAPK	mitogen activated kinase-like protein
NF κ B	nuclear factor kappa B
MyD88	myeloid differentiation primary response gene
mRNA	messenger ribonucleic acid
CD14	monocyte differentiation antigen
LPS	lipopolysaccharide
TNF α	tumor necrosis factor α
IL-1 β	interleukin 1 beta
CD	chow diet
PAMPs	pathogen-associated molecular patterns

1. Introduction

Non-alcoholic fatty liver disease (NAFLD) is a common chronic liver disease characterized by fatty degeneration of the liver more than 5 % without specific factors. The disease spectrum includes nonalcoholic fatty liver disease (NAFL), nonalcoholic steatohepatitis (NASH), cirrhosis, and hepatocellular carcinoma (HCC). The prevalence of NAFLD around the world is 13.00 %–30.45 %, with an average of about 25.00 % [1,2]. NAFLD is the most common chronic liver disease in Western countries, and its incidence rate in Asia is also increasing year by year [3]. The pathogenesis and mechanism of NAFLD has not yet been clarified. The mainstream hypothesis of pathogenesis has developed from the traditional “two-hit” theory to the “multiple-hit” theory, which refers to many harmful factors including genetic and environmental factors that hit the liver at the same time [4]. NAFLD is a multi-system disease, usually accompanied by obesity, metabolic syndrome, insulin resistance, type 2 diabetes (T2DM), and other metabolic abnormalities. And in the course of the disease, it will damage multiple extrahepatic organs and metabolic processes, increasing the risk of cardiovascular disease and kidney disease [5]. Generally, NAFLD patients die of extrahepatic complications, mainly cardiovascular disease [5]. At present, the gold standard for the diagnosis of NAFLD is liver biopsy. However, due to the absence of obvious symptoms of early NAFLD and the consideration of the invasive nature of biopsy, this examination method is not widely used in clinical practice. The most used diagnostic method is liver ultrasound, but liver steatosis of less than 20 %–30 % is difficult to detect due to its sensitivity [6]. At present, there is no specific drug approved for NAFLD. The mainstream treatment plan is to change lifestyle, adjust diet structure, control excessive fructose and fat intake, increase physical exercise, etc., supplemented with certain liver protection drugs, and treat complications. Therefore, the search for drugs targeting NAFLD has become the focus of researchers in recent years.

Acetylation modification is a common and important post-translation regulation mode of proteins, and the acetylation balance of histones affects gene expression, which is regulated by histone acetylase and histone deacetylase (HDAC). HDACs are a class of proteins with deacetylation activity, which can remove the ϵ -acetyl group on histones acetyl-lysine and were first found in calf thymus extract in 1969 [7]. At present, a total of 18 HDACs have been found in mammals, which are divided into two families and four categories, and are named HDAC1-11 and SIRT1-7 according to the order of discovery. HDACs not only have enzymatic activity on histones but also have a regulatory effect on many non-histones. HDACs are widely distributed in different tissues and different substructures of cells in the body, participate in many important metabolic processes and play a unique role in the pathogenesis and development of various diseases [8]. HDACs inhibitor (HDACi) is a kind of natural or artificial small-molecular substance with deacetylation inhibition activity, which can combine with HDACs and inhibit their enzyme activity and has special effects in tumor treatment. HDACs are also involved in the pathogenesis and development of NAFLD [9]. Zinc finger protein Snail1 can inhibit the expression of adipogenic genes in liver cells, antagonize insulin induced hepatic steatosis, and its normal function depends on the normal function of HDAC1/2 [10]. HDAC2 has also been reported to be involved in the progression of NAFLD to cirrhosis [11]. HDAC3 has been found to participate in liver lipid metabolism through co-repressor complexes, which have been reported to inhibit fat generation and promote fatty acid oxidation [12]. And another subunit of the complex, G protein pathway inhibitor 2, has been reported to play a central role in the progression of NAFL to NASH [13]. In the SIRT family of Class III HDACs, SIRT1, 2, and 3 have been reported as potential targets for the treatment of NAFLD [14–19]. HDAC11 is believed to be related to the metabolism and thermogenic processes of adipose tissue, some scholars believe that inhibiting the function of HDAC11 can reverse liver steatosis and may be an important target for treating NAFLD [20,21]. Therefore, using HDACi to intervene in NAFLD has also become one of the new directions. ACY-1215 is an oral and effective HDAC6 selective inhibitor, which has shown satisfactory safety and efficacy in clinical and preclinical trials of various

diseases such as tumors, osteoarthritis, acute liver injury, and acute liver failure [22–27]. Especially in the model of acute liver injury, ACY-1215 can protect hepatocytes in different mechanisms [27–29], Chen et al. reported that ACY-1215 can inhibit the activation of NLRP3 inflammasomes, inhibit the apoptotic signaling pathway, and thus improve acute liver injury [27]; Zhang et al. reported that ACY-1215 can inhibit the activation of the TLR4/MAPK/NFκB pathway in macrophages, directly reducing inflammatory activation in acute liver injury models [28]; Wang et al. reported that ACY-1215 can inhibit the activation of M1 macrophages, thereby protecting acute liver injury model mice [29]. We believe that ACY-1215 also has therapeutic potential for NAFLD, so we preliminarily explore the effect of ACY-1215 on NAFLD and its mechanism through TMT relative quantitative proteomics.

2. Materials and methods

2.1. Cell model

AML-12 cell line and MIHA cell line were used. Oleic acid (OA) and palmitic acid (PA) were mixed in a 2:1 ratio for the construction of the NAFLD model. An appropriate concentration of mixed fatty acids (250 μmol/L OA+125 μmol/L PA for AML 12 cells and 125 μmol/L OA+62.5 μmol/L PA for MIHA cells) was added to the culture medium and was incubated for 24 h, then replaced with fresh medium with 1 μg/L lipopolysaccharide (LPS) incubated for 24 h. Meanwhile corresponding concentrations of ACY-1215 (Selleck, Houston, USA, 1 μM, 5 μM, 10 μM, 20 μM) was added to ACY-1215 treatment group incubated for 24 h.

2.2. Animal model

C57BL/6J male mice were used (Experimental animals purchased from the Department of Experimental Zoology of Xiangya Medical College). After a week of adaptive feeding, they were randomly divided into a blank control group, a negative control group, a model group, a solvent control group, and 3 ACY-1215 treatment groups (ACY-1215 concentrations were 10, 30, and 50 mg/kg, respectively), each group contains 5 mice. The blank control group and the negative control group were given a chow diet (CD), and the other groups were given a high-fat diet (HFD) (Research Diets: D09100319) for a total of 16 weeks. In the 8–16 week, the blank control group was given the saline intraperitoneal injection, the solvent control group was given the solvent intraperitoneal injection, and the negative control group and the ACY-1215 treatment group were given ACY-1215 intraperitoneal injection of corresponding concentration. The solvent composition is 5 % DMSO+60 % PEG300 + 35 % ddH₂O. The experimental animals were then euthanized, and serum and liver samples were taken. Animal ethics has been approved by the Experimental Animal Ethics Committee of Xiangya Medical College (CSU-2022-0033).

2.3. TMT relative quantitative proteomics

2.3.1. Protein extraction and TMT labeling

Cells were lysed and protein extracted using SDT buffer (4 % SDS, 100 mmol/L Tris-HCl, 1 mmol/L DTT, pH 7.6). The protein content was quantified using a BCA kit (NCM Biotech, Suzhou, China). The sample is then labeled using a TMT labeling kit (Thermo Scientific, Massachusetts, USA). According to the instructions provided by the manufacturer, use TMT reagent to label 100 μg peptide segment mixture samples in each group.

2.3.2. High pH reversed-phase fractionation

The labeled peptide segments were separated using a high pH reverse phase peptide segment separation kit (Thermo Scientific, Massachusetts, USA). First, column equilibrium was performed with acetonitrile and 0.1 % trifluoroacetic acid. The labeled sample was loaded and centrifuged at low speed. The peptide segments bound to the column were then gradient eluted using a high pH acetonitrile solution with sequentially increasing concentrations. Then, the sample was vacuum dried and redissolved with 12 μl 0.1 % TFA solution. The absorbance at 280 nm was measured, and the peptide concentration was calculated.

2.3.3. LC-MS/MS analysis

LC-MS/MS analysis was performed on a Q Exactive mass spectrometer (Thermo Scientific, Massachusetts, USA) that was coupled to Easy nLC (Proxeon Biosystems, now Thermo Scientific) for 60/90 min. Buffer A used is a 0.1 % formic acid aqueous solution, and buffer B is a 0.1 % formic acid acetonitrile aqueous solution, with an acetonitrile concentration of 84 %. The chromatographic column is balanced with 95 % buffer A, and the sample is loaded into the sample loading column (Thermo Scientific Acclaim PepMap 100, 100 μm*2 cm, nanoViper C18). A flow rate of 300 nl/min was used for separation through an analytical column (Thermo Scientific EASY column, 10 cm, ID 75 μm, 3 μm, C18-A2). After chromatographic separation, the sample was analyzed by mass spectrometry using a Q-Exactive mass spectrometer.

2.3.4. Protein identification and quantification

The MASCOT engine (Matrix Science, London, UK; version 2.2) and Proteome Discover 1.4 software was used to search the RAW files of mass spectrometry analysis for protein identification and quantitative analysis.

2.3.5. Bioinformatics analysis

The STRING database was used to analyze differentially expressed proteins and obtain protein interaction networks. Nodes that are

not in the network were excluded. The k means method in cluster was used to analyze the network. Then retrieved and analyzed annotations of Gene Ontology (GO) database and Kyoto Encyclopedia of Genes and Genomes (KEGG) database involved in the cluster where the hot spot proteins are located.

2.4. Oil red O staining

Cells were stained in Petri dishes with oil red O. The samples were incubated with 4 % paraformaldehyde for 5 min, soaked in PBS buffer, then oil red O staining solution was added to soak for 5 min, and then decolorized with 60 % isopropanol aqueous solution for 3–5 min. Images were collected under an inverted microscope. Oil red O staining was performed after the animal liver was made into a frozen section. After rewarming, the slices were soaked in oil red O staining solution for 8–10 min, then dipped in 60 % isopropanol aqueous solution for 3 s and 5 s and dipped in pure water for 10 s in between. Then soaked the slices in hematoxylin staining solution for 3–5 min, and soaked in pure water for 5 s, 10 s, and 30 s respectively. The slices were added into blue solution for 2–8 s, and soaked in pure water for 5 s and 10 s. The microscope then observes and captures images.

2.5. Eosin hematoxylin (HE) staining

Animal livers were made into paraffin sections for HE staining. The slices were placed in xylene I for 20 min, in xylene II for 20 min, in absolute ethanol I for 5 min, in absolute ethanol II for 5 min, and in 75 % ethanol in water for 5 min. After gently rinsed the sections with water, soaked them in a hematoxylin staining solution for 3–5 min, and then gently rinsed with water. Sections were sequentially dehydrated in 85 % and 95 % aqueous ethanol and then immersed in eosin staining solution for 5 min. The stained sections were dehydrated in absolute ethanol I for 5 min, in absolute ethanol II for 5 min, in absolute ethanol III for 5 min, in xylene I for 5 min, and in xylene II for 5 min. Finally, observed under a microscope and captured images.

2.6. Detection of TG, AST, and ALT

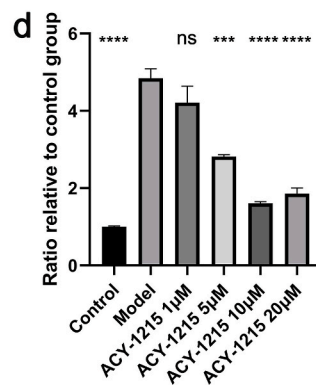
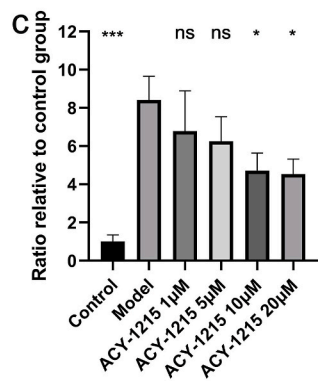
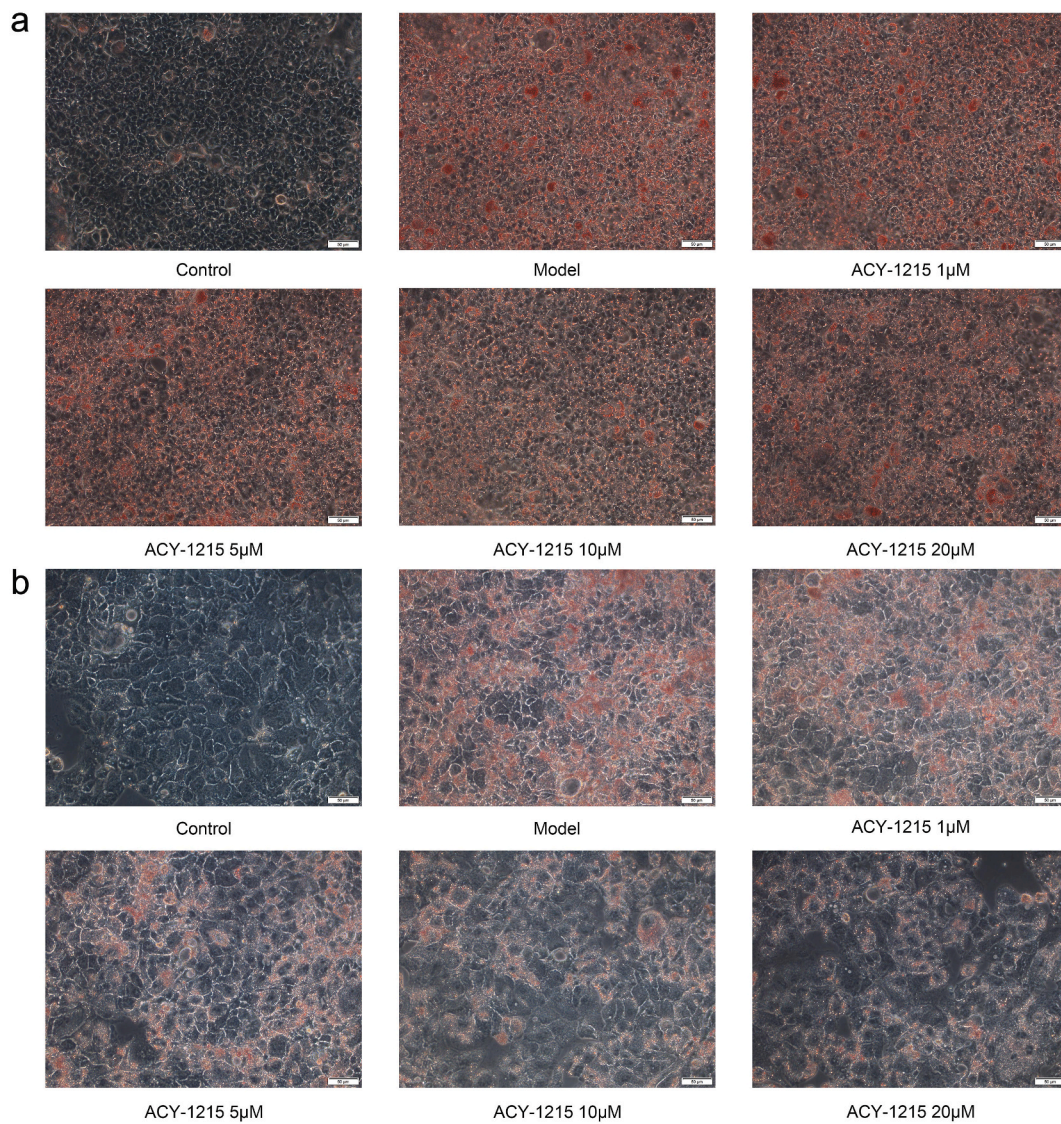
An appropriate number of broken cells or serum was diluted for testing, and the TG test kit (Jiangcheng, Nanjing, China) was used to process the sample before measuring the absorbance at 510 nm. Dilute an appropriate number of broken cells or serum for testing, use the AST test kit (Jiangcheng, Nanjing, China) to process the sample, and measure the absorbance at 510 nm. An appropriate number of broken cells or serum was diluted for testing, and the ALT test kit (Jiangcheng, Nanjing, China) was used to process the sample before measuring the absorbance at 510 nm. The specific sample processing method can be found in the kit manual.

2.7. Fluorescent quantitative PCR (qPCR)

RNAiso PLUS reagent was used to crush cells or liver tissue, and chloroform, isopropanol, and absolute ethanol was used to extract RNA. A one-step gDNA removal and cDNA synthesis kit (TransGen Biotech, Beijing, China) was used for reverse transcription. After measuring the RNA concentration, a total of 5 µg RNA was taken and a 20 µl reaction system was prepared according to the

Table 1
Primer sequence table.

Gene Name	Sequence (5'→3')
m-CD14-F	CTCTGTCCCTTAAAGCGGCTTAC
m-CD14-R	GTTGCGGAGGTTCAAGATGTT
m-TLR4-F	GCCCTACCAAGTCTCAGCTA
m-TLR4-R	CTGCAGCTCTTCTAGACCCA
m-MYD88-F	TCATGTTCTCCATACCCTTGGT
m-MYD88-R	AAACTGCGAGTGGGGTCAG
m-IL-1β-F	TCAGGCAGGCAGTATCACTC
m-IL-1β-R	AGCTCATATGGGTCCGACAG
m-TNF-α-F	CGTCAGCCGATTTGCTATCT
m-TNF-α-R	CGGACTCCGCAAAGTCTAAG
m-GAPDH-F	ATGGGTGTGAACCACGAGA
m-GAPDH-R	CAGGGATGATGTTCTGGGCA
h-CD14-F	ACGCCAGAACCCTGTGAGC
h-CD14-R	GCATGGATCTCCACCTCTACTG
h-TLR4-F	AGACCTGTCCCTGAACCCCTAT
h-TLR4-R	CGATGGACTTCTAAACCAGCCA
h-myd88-F	GGCTGCTCTCAACATGCGA
h-myd88-R	CTGTGTCCGACGTTCAAGA
h-IL-1β-F	ATGATGGCTTATTACAGTGGCAA
h-IL-1β-R	GTGGAGATTCTGAGCTGGA
h-TNF-α-F	GAGGCCAAGCCCTGGTATG
h-TNF-α-R	CGGGCCGATTGATCTCAGC
h-GAPDH-F	GGAGCGAGATCCCTCCAAAAT
h-GAPDH-R	GGCTGTTGCATACTTCTCATGG



(caption on next page)

Fig. 1. ACY-1215 attenuates lipid accumulation in NAFLD cell model (The model group only received fatty acid intervention). a: Oil red O staining results in AML-12 cell model of NAFLD under different conditions. b: Oil red O staining results in the MIHA cell model of NAFLD under different conditions. c: Comparison of triglyceride content in AML-12 cell model of NAFLD under different conditions. d: Comparison of triglyceride content in MIHA cell model of NAFLD under different conditions. ns, not statistically significant; * $P < 0.05$; ** $P < 0.01$; *** $P < 0.001$; **** $P < 0.0001$. $n = 3$. (All comparisons between the model group and other groups.). (For interpretation of the references to color in this figure legend, the reader is referred to the Web version of this article.)

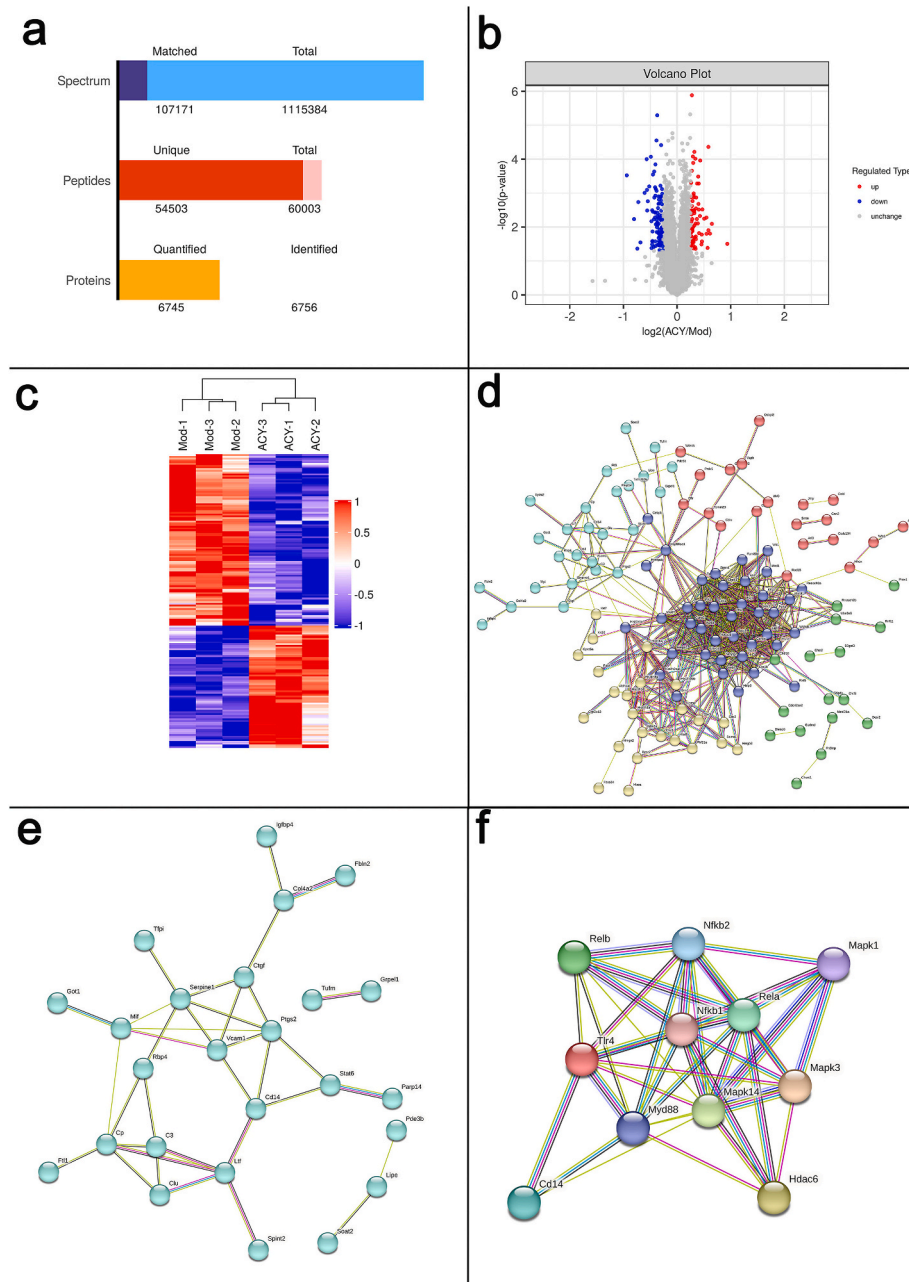


Fig. 2. Proteomics analysis and protein interaction network. a: Number of identified peptides and proteins. b: Volcano plot of differential proteins. c: Cluster analysis of differential proteins. d: Differentially expressed protein interaction network between model group and ACY-1215 treatment group. e: A cluster of differentially expressed protein interaction networks comprising CD14. f: Prediction of the interaction network between CD14 and TLR4/MyD88/MAPK/NF κ B pathway-related proteins.

instructions. The system was placed on a gradient PCR instrument and reverse transcription was performed according to the conditions set in the kit instructions. 80 μ l enzyme-free water was used to dilute cDNA, performed qPCR using a dye-based fluorescence quantitative premix kit (TransGen Biotech, Beijing, China), a 10 μ l reaction system was prepared according to the instructions, the system was placed on a fluorescence quantitative PCR instrument, and amplification curve data and melting curve data was obtained according to the instructions. The primers used are shown in [Table 1](#).

2.8. Western blotting (WB)

Protease inhibitors and RIPA lysate was mixed at a ratio of 1:100 to disrupt cells and liver tissue and to extract proteins from cells and liver tissue. The BCA kit was used to measure the protein concentration, and PBS buffer and the loading reagent was used to adjust the protein concentration. The separating gel and stacking gel with a concentration of 6%–10 % were prepared according to the instructions of the rapid gel preparation kit (Biosharp, Hefei, China). Marker and the sample protein to be tested was added into the sample well, then performed vertical electrophoresis. Proteins were then transferred from the SDS-PAGE gel to PVDF membranes (BIO-RAD, California, USA). Skim milk (Biosharp, Hefei, China) was used to block the PVDF membrane, then the samples were incubated in the corresponding primary antibody and incubated at 4 °C on a horizontal shaker for 12–16 h. TBST buffer was used for washing, and then the samples were incubated in the corresponding secondary antibody for 60 min. Chemiluminescent visualization was performed after washing with TBST buffer.

2.9. Statistical analysis

Using GraphPad Prism 8 for statistical analysis. The Student T-test was performed on continuous variable data, and the data were expressed as mean \pm standard deviation. N represents the data sample size, and $P \leq 0.05$ is considered statistically significant. All experiments were independently repeated more than 3 times.

3. Results

3.1. ACY-1215 has a protective effect on the NAFLD cell model

We used different concentrations of fatty acids to establish NAFLD cell models, then added ACY-1215 for 24 h of treatment and used Oil Red O staining and TG assay kits to detect the effect of ACY-1215 on lipid accumulation in NAFLD cell models. In AML-12 cells and MIHA cells, mixed fatty acids could cause excessive accumulation of intracellular lipids, resulting in fatty degeneration of cells ([Fig. 1a](#) and [b](#)). Adding different concentrations of ACY-1215 for intervention, fat accumulation, and steatosis caused by fatty acids would be significantly reduced ([Fig. 1a](#) and [b](#)). We further measured the TG content in the cells, and the results were similar to Oil Red O staining. The mixed fatty acids could significantly increase the TG content in the cells. After the intervention of ACY-1215, this increase would be inhibited ([Fig. 1c](#) and [d](#)). We can find out that ACY-1215 had a protective effect on the cell model of NAFLD from the above results.

3.2. ACY-1215 may exert a protective effect on the AML-12 cell model of NAFLD by inhibiting the expression level of CD14

To explore the mechanism of the protective effect of ACY-1215 on the cell model of NAFLD, we conducted the TMT relative proteomic detection on the model group and the ACY-1215 treatment group of the AML-12 cell model. The sample parameters were compared with the data in the database, and finally, 10,717 secondary spectrum data were matched, and 60,003 peptides and 6756 proteins were identified, of which 6745 were quantifiable proteins ([Fig. 2](#)). Taking the expression fold up-regulation greater than 1.2 times or down-regulation less than 0.83 times and $P < 0.05$ as the standard, a total of 168 differentially expressed proteins were obtained between the model group and the ACY-1215 treatment group, of which 70 proteins were up-regulated and 98 proteins were down-regulated in the ACY-1215 treatment group. All differentially expressed proteins were analyzed by the protein interaction network through the STRING database, and cluster analysis was performed on the protein interaction network, and the hotspot proteins in the results were retrieved and analyzed ([Fig. 2](#)). We found that the expression of CD14 in the ACY-1215 treatment group was decreased significantly, which is related to the Toll-like receptor pathway and NF κ B pathway. At the same time, studies have reported that the increased expression of CD14 may be related to the pathogenesis and development of NAFLD. Therefore, we analyzed the interaction of HDAC6, CD14, and related proteins in the TLR4/MyD88/MAPK/NF κ B signaling pathway through the STRING database. The results indicate that there is an interaction between HDAC6, CD14, and related proteins in the TLR4/MyD88/MAPK/NF κ B signaling pathway ([Fig. 2c](#)). These results showed that ACY-1215 may reduce the expression level of CD14, inhibit the activation of the TLR4/MyD88/MAPK/NF κ B signaling pathway, and produce a protective effect on NAFLD. However, the expression levels of TLR4 and MyD88 did not change significantly between the model group and the ACY-1215 treatment group, and the active forms of key proteins in the MAPK pathway and NF κ B pathway were phosphorylated, the change levels could not be measured by this method. Therefore, we would activate the CD14/TLR4/MyD88/MAPK/NF κ B signaling pathway by adding exogenous LPS stimulation to the NAFLD cell model and test the effect of ACY-1215 on the NAFLD cell model again.

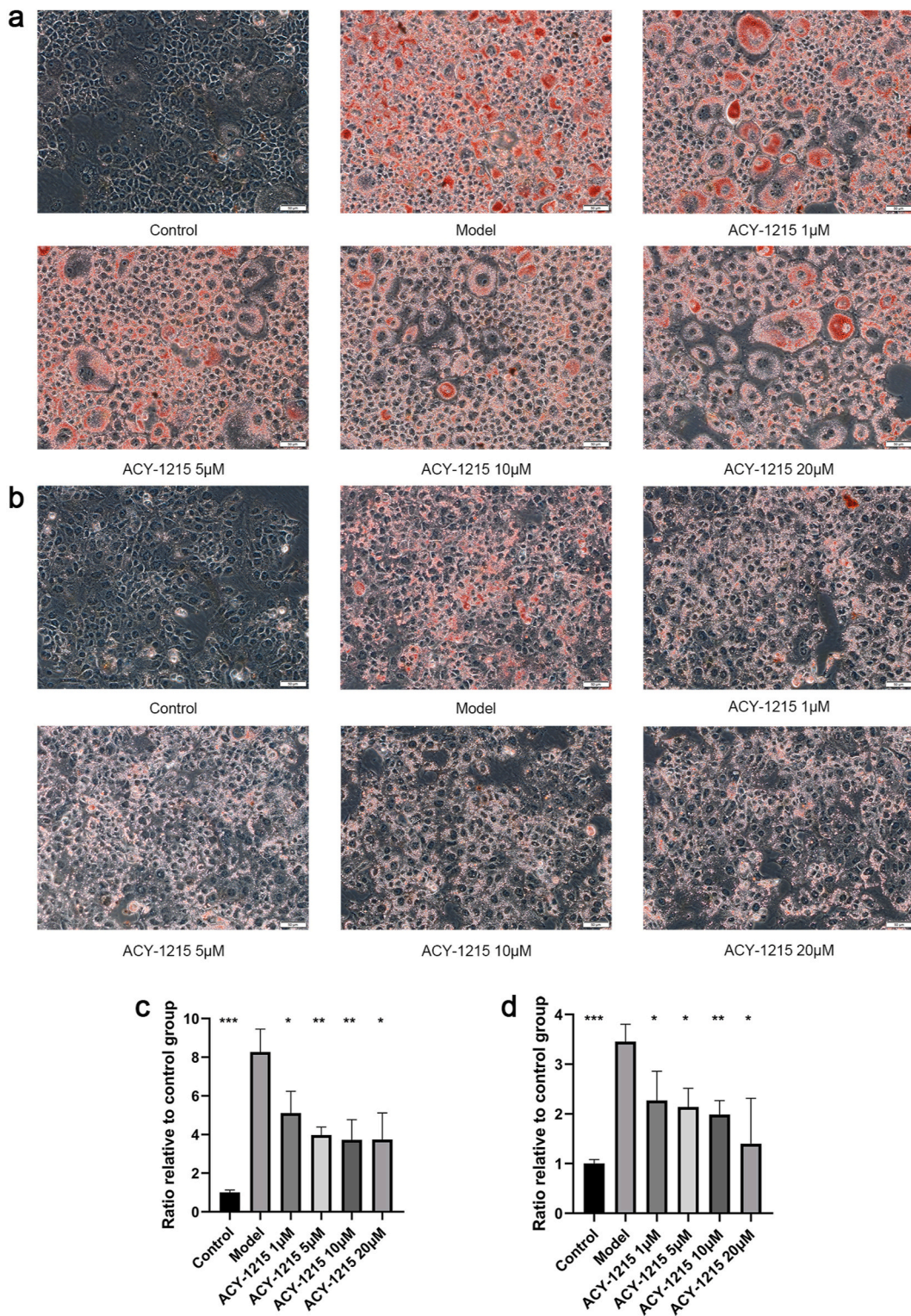


Fig. 3. ACY-1215 attenuates lipid accumulation in NAFLD cell model (The model group received fatty acid and LPS intervention).

a: Oil red O staining results in AML-12 cell model of NAFLD under different conditions. b: Oil red O staining results in the MIHA cell model of NAFLD under different conditions. c: Comparison of triglyceride content in AML-12 cell model of NAFLD under different conditions. d: Comparison of triglyceride content in MIHA cell model of NAFLD under different conditions. ns, not statistically significant; * $P < 0.05$; ** $P < 0.01$; *** $P < 0.001$; **** $P < 0.0001$. $n = 3$. (All comparisons between the model group and other groups.) (For interpretation of the references to color in this figure legend, the reader is referred to the Web version of this article.)

3.3. ACY-1215 has protective effects on NAFLD cell models and animal models

Combining the above results, we decided to use LPS as an additional stimulus in the cellular model of NAFLD, and at the same time, supplement the results of animal models of NAFLD as further evidence. In AML-12 and MIHA cell models, ACY-1215 still has a protective effect on NAFLD cell models under the premise of LPS as an additional stimulus (Fig. 3).

We induced a mouse model of NAFLD using HFD and intervened with ACY-1215. HFD could significantly increase the body weight of mice, and at the same time, significant fatty degeneration occurs in the liver of mice, and the levels of AST, ALT, and TG in serum also

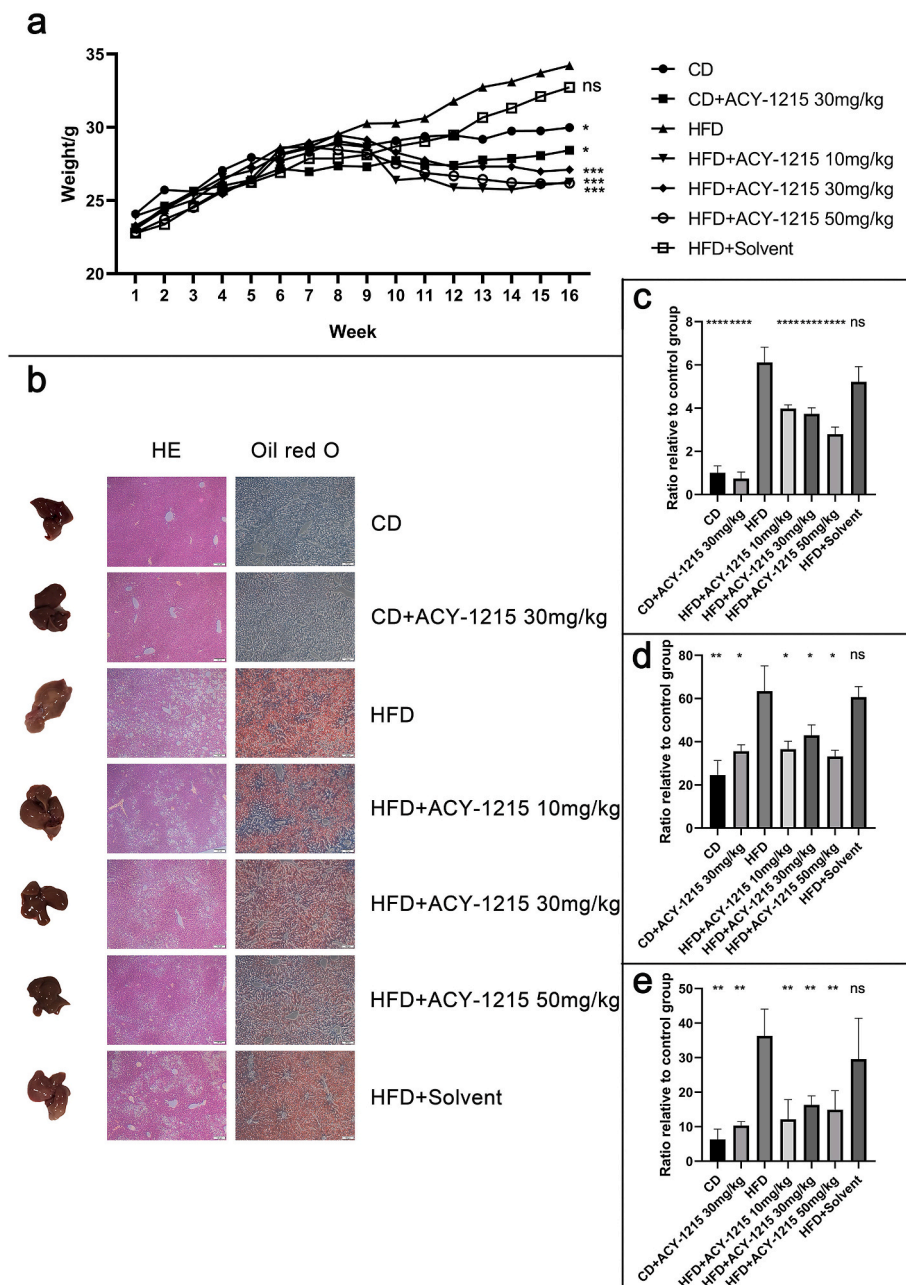


Fig. 4. ACY-1215 is protective in the C57 mouse model of NAFLD.

a: Body weight changes of C57 mice during the experiment. b: Liver specimens, liver HE stained sections and Oil Red O-stained sections of different groups of C57 mice. c: Comparison of AST content in serum of C57 mice in different groups. d: Comparison of ALT content in serum of C57 mice in different groups. e: Comparison of TG content in serum of C57 mice in different groups. ns, not statistically significant; *P < 0.05; **P < 0.01; ***P < 0.001; ****P < 0.0001. n = 5. (All comparisons between the model group and other groups.) (For interpretation of the references to color in this figure legend, the reader is referred to the Web version of this article.)

significantly increase (Fig. 4). After the intervention of ACY-1215, the body weight of the mice in the treatment group decreased significantly after the intervention, and then gradually stabilized at a level significantly lower than that of the model group (Fig. 4a). At the same time, the degree of fatty degeneration in the liver partially improved, and the cavities and oil red O dye in the liver slices were reduced compared with the model group (Fig. 4b). In the serum, the levels of AST, ALT, and TG in the mice in the treatment group were also significantly lower than those in the model group (Fig. 4c–e). The above results indicated that after HFD induction, hepatic parenchymal cells of C57 mice were also damaged, fatty degeneration occurred in the liver, and liver enzymes released into the serum increased correspondingly. The intervention of ACY-1215 could alleviate the fatty degeneration of the liver and reduce the damaged hepatic parenchymal cells, that is, ACY-1215 could alleviate the onset and progression of NAFLD to a certain extent.

3.4. ACY-1215 had a protective effect on the experimental model of NAFLD by inhibiting the activation of CD14/TLR4/MyD88/MAPK/NFκB pathway

We verified the mRNA changes of some proteins related to the CD14/TLR4/MYD88 pathway under different conditions in the cell and animal models of NAFLD. Meanwhile, we also detected the mRNA expression of downstream inflammatory factors IL-1β and TNFα after the activation of the MAPK/NFκB signaling pathway. The results showed that the mRNA levels of CD14, TLR4, and MyD88 in the model group were significantly increased under the stimulation of the modeling conditions. At the same time, the mRNA expression

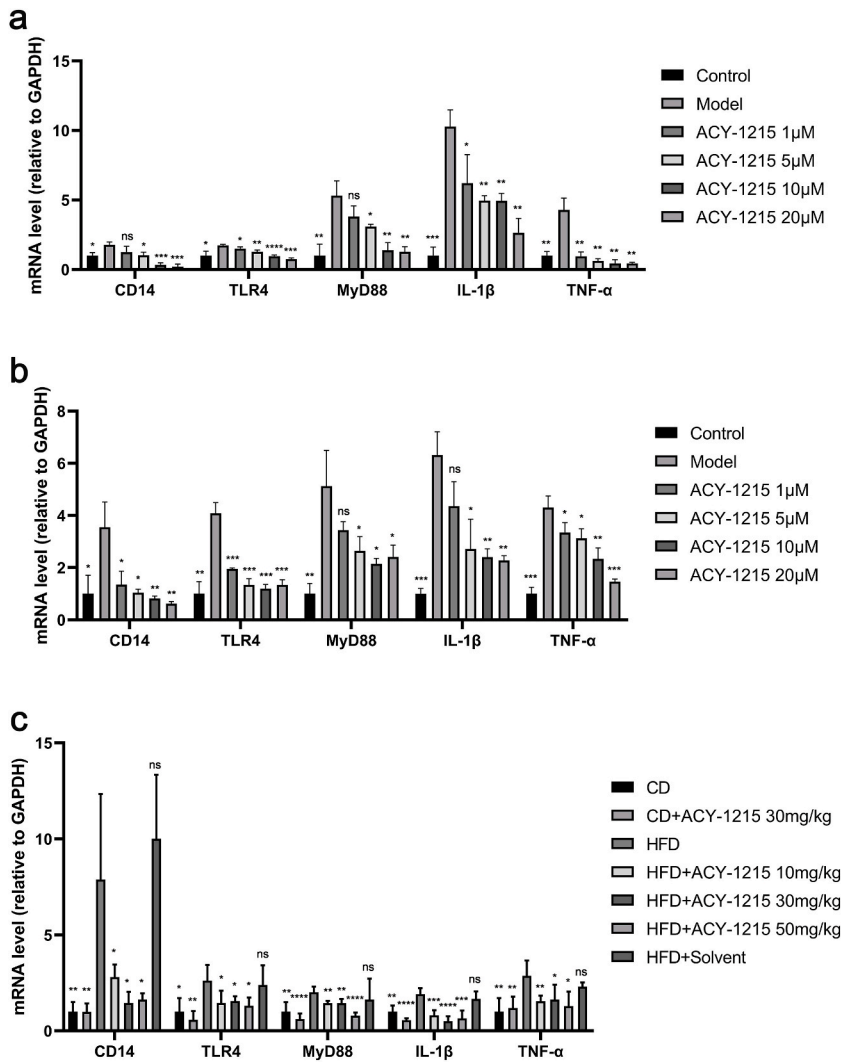


Fig. 5. Comparison of mRNA levels of CD14, TLR4, MyD88, IL-1β and TNF-α in different models. a: Comparison of mRNA levels of CD14, TLR4, MyD88, IL-1β and TNF-α in AML-12 cell model of NAFLD. b: Comparison of mRNA levels of CD14, TLR4, MyD88, IL-1β and TNF-α in MIHA cell model of NAFLD. c: Comparison of mRNA levels of CD14, TLR4, MyD88, IL-1β and TNF-α in C57 mice model of NAFLD. ns, not statistically significant; *P < 0.05; **P < 0.01; ***P < 0.001; ****P < 0.0001. n = 3 in cell model, n = 5 in mice model. (All comparisons between the model group and other groups.)

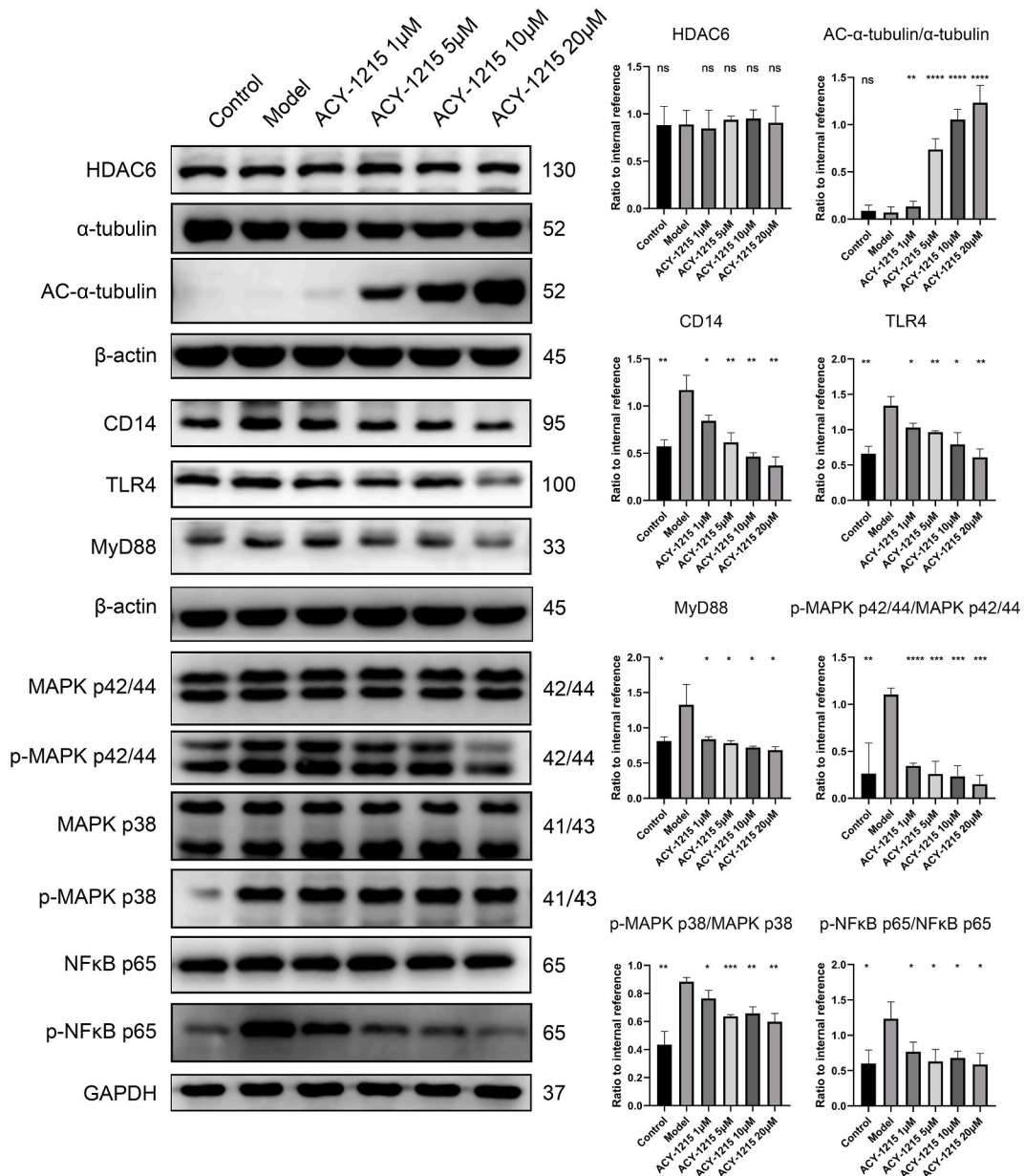


Fig. 6. ACY-1215 can inhibiting the activation of CD14/TLR4/MyD88/MAPK/NFκB signal pathway in AML-12 cell model of NAFLD. ns, not statistically significant; *P < 0.05; **P < 0.01; ***P < 0.001; ****P < 0.0001. n = 3. (All comparisons between the model group and other groups.)

levels of inflammatory factors IL-1β and TNF-α also increased significantly (Fig. 5). After the intervention of ACY-1215, the increase of the above-mentioned mRNA expression level could be partially inhibited (Fig. 5). Further, we detected the expression levels of the corresponding proteins. In cell models and animal models, the expression levels of CD14, TLR4, and MyD88 were significantly increased in the model group, while this increase was inhibited in the ACY-1215 treatment group (Figs 6–8). In the MAPK\NFκB pathway, we detected the total amount and phosphorylation level of MAPK p38, MAPK p42/44, and NFκB p65. In the model group, the total levels of MAPK p38, MAPK p42/44, and NFκB p65 did not change significantly, but their phosphorylation levels increased significantly (Figs. 6–8). After the intervention of ACY-1215, the increase of the phosphorylation level of the above-mentioned proteins was inhibited to varying degrees (Figs. 6–8). In summary, ACY-1215 could inhibit the expression levels of CD14, TLR4, and MyD88 in NAFLD cells and animal models, and inhibit the activation level of the MAPK/NFκB pathway, thereby exerting a protective effect on NAFLD models.

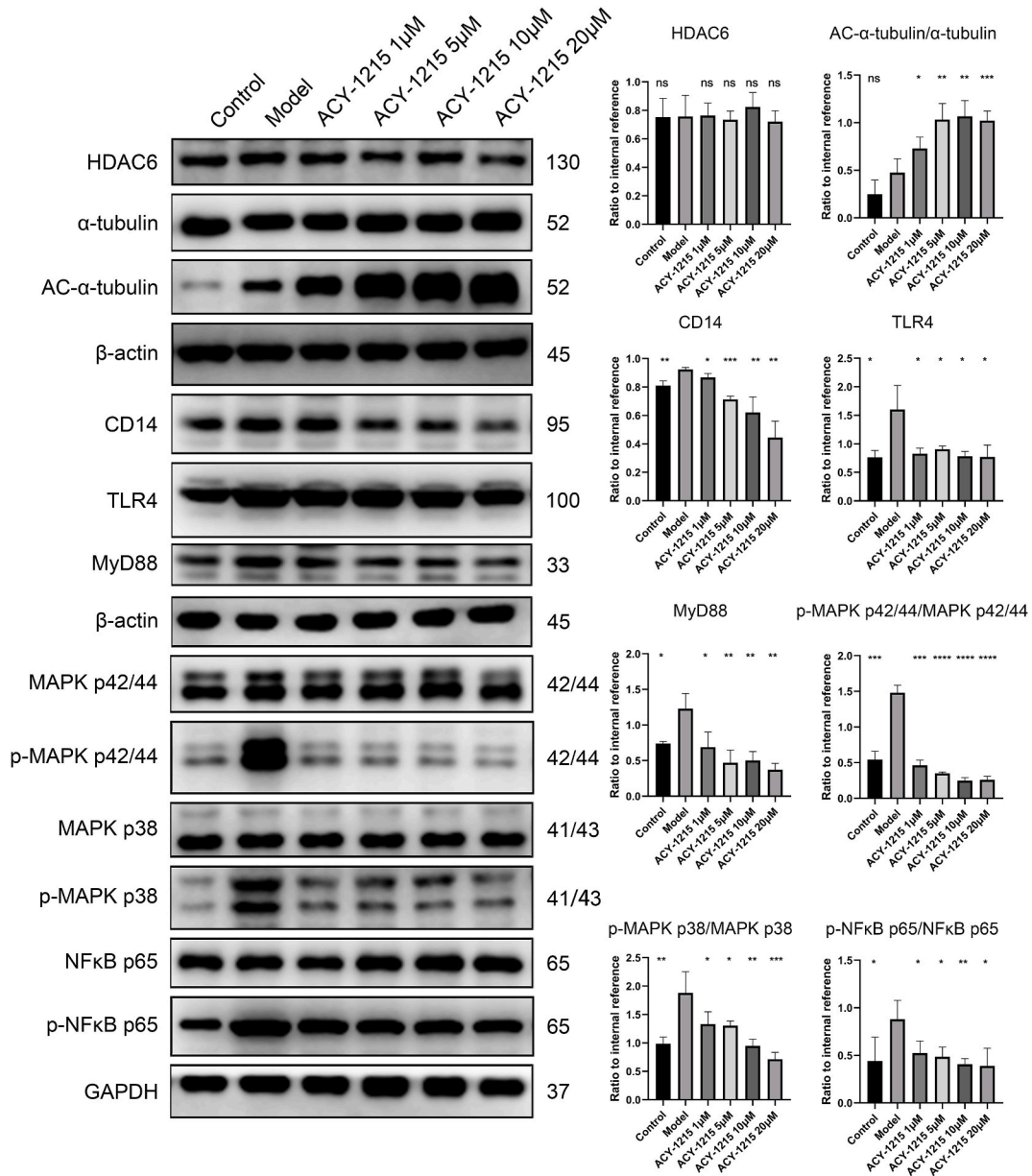


Fig. 7. ACY-1215 can inhibiting the activation of CD14/TLR4/MyD88/MAPK/NFκB signal pathway in MIHA cell model of NAFLD. ns, not statistically significant; * $P < 0.05$; ** $P < 0.01$; *** $P < 0.001$; **** $P < 0.0001$. $n = 3$. (All comparisons between the model group and other groups.)

4. Discussions

NAFLD is one of the main causes of chronic liver disease worldwide. It is closely related to the high-fat diet, obesity, type 2 diabetes, hyperlipidemia, insulin resistance, and metabolic syndrome, but its exact pathogenesis has not yet been clarified. The incidence rate of NAFLD worldwide is about 25.00 %, and it has become the main indication of liver transplantation, which has brought a serious economic burden to patients and society [1]. At present, there is no specific treatment plan or medication for NAFLD. Therefore, exploring the pathogenesis of NAFLD and searching for possible therapeutic targets to alleviate disease progression or even reverse the onset process is currently a hot topic and focus of research. HDACs can regulate gene expression and participate in a variety of metabolic processes and the occurrence and development of diseases, including NAFLD [8,9]. Inhibitors targeting HDACs are ideal intervention methods, and among many HDACi, selective inhibitors are a better choice. ACY-1215 is the first oral effective selective inhibitor of HDAC6, with a semi-inhibitory concentration of 4.7 nmol/L, and has achieved satisfactory therapeutic effects in preclinical and clinical trials of various diseases [30]. In liver diseases, ACY-1215 has protective effects on acute liver injury.

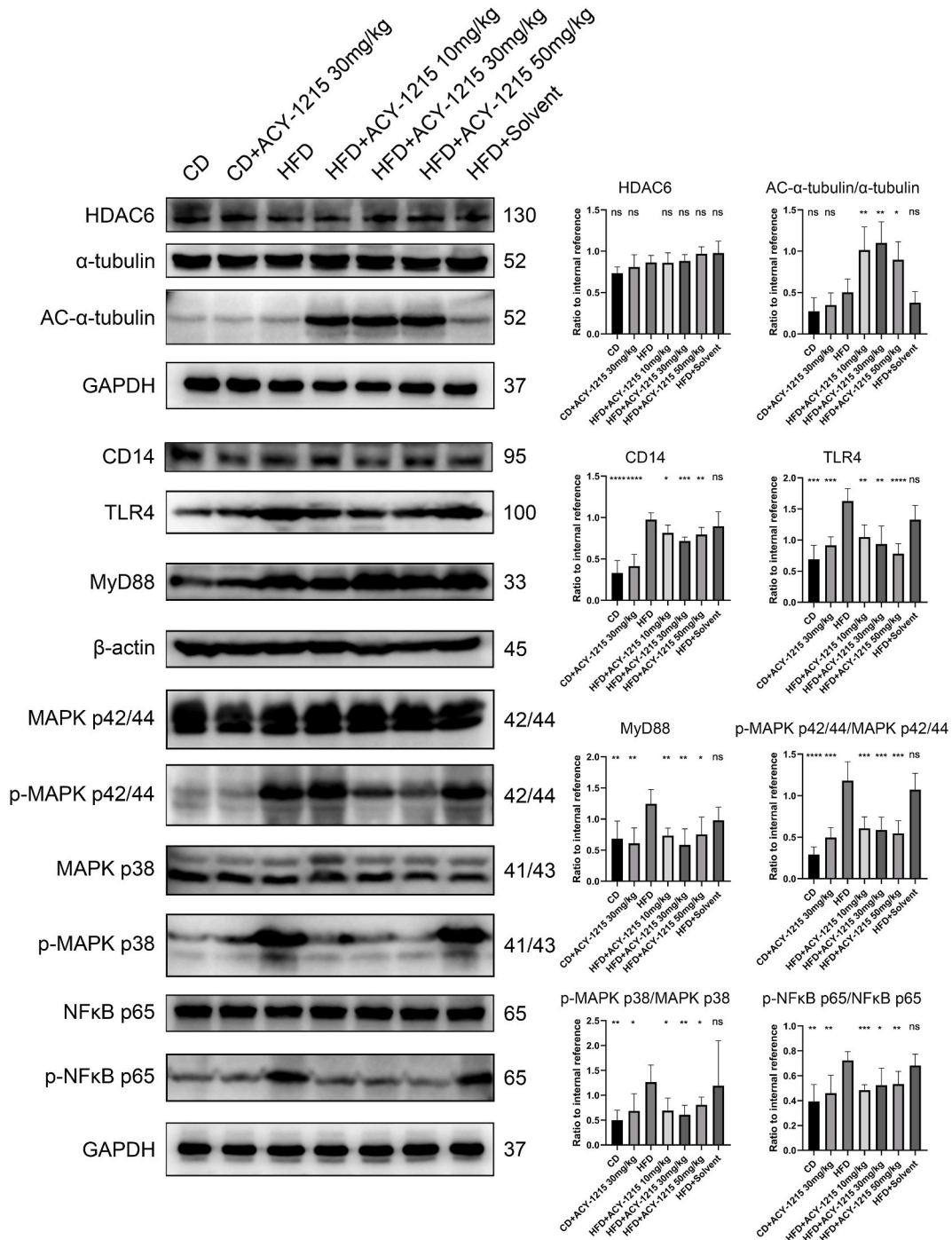


Fig. 8. ACY-1215 can inhibiting the activation of CD14/TLR4/MyD88/MAPK/NFκB signal pathway in C57 mice model of NAFLD. ns, not statistically significant; *P < 0.05; **P < 0.01; ***P < 0.001; ****P < 0.0001. n = 5. (All comparisons between the model group and other groups.)

This study established cellular and animal models of NAFLD using AML-12 cells, MIHA cells, and C57 mice and intervened with ACY-1215 in these models. We found that ACY-1215 can alleviate lipid accumulation and steatosis in liver cells under conditions of excessive fat intake, and significantly reduce intracellular fat vacuoles and TG content. In vivo experiments, ACY-1215 can reduce the weight gain of experimental animals, excessive fat accumulation in the liver, and the rise of AST, ALT, and TG levels in serum induced by HFD. Furthermore, by detecting the mRNA expression levels of related inflammatory factors in liver cells, it was found that ACY-1215 can inhibit the increase in transcription levels of inflammatory factors in the liver in the NAFLD model. The above findings

suggest that ACY-1215 has a protective effect on NAFLD under both in vitro and in vivo conditions. To explore the mechanism of the protective effect of ACY-1215 on the NAFLD experimental model, we carried out a TMT relative proteomics test on the AML-12 cell model. In the differentially expressed proteins between the model group and the ACY-1215 treatment group, we found a decrease in CD14 expression in the ACY-1215 treatment group. Using the CLUSTER database, we found a possible interaction between CD14 and the TLR4/MyD88/MAPK/NF κ B signaling pathway. Furthermore, we identified the CD14/TLR4/MyD88/MAPK/NF κ B signaling pathway in the KEGG database, which is involved in mediating the innate immune response mechanism of cells to LPS. It is worth noting that in in vitro experiments when we performed the TMT relative proteomics test, the modeling condition was only the stimulation of mixed fatty acids. Under this condition, the expression levels of TLR4 and MyD88 in the ACY-1215 treatment group were not significantly different from those in the model group. Then, we further tested in the blank control group and the model group, and the expression levels of TLR4 and MyD88 were not significantly different. We speculate that this is due to the lack of LPS stimulation in liver cells under in vitro conditions, where the activation level of the CD14/TLR4/MyD88/MAPK/NF κ B signaling pathway did not reach its peak and ACY-1215 inhibited the expression of membrane receptor CD14, resulting in no significant difference in the expression levels of TLR4 and MyD88 between the groups in the results. In vivo experiments, there is a natural bacterial community in the intestines of experimental animals, and under the induction of HFD, intestinal barrier dysfunction occurs, allowing LPS in the intestine to reach the liver through blood circulation. This speculation was confirmed in subsequent experiments. After adding LPS as an additional stimulus in vitro experiment, the levels of TLR4 and MyD88 in liver cells significantly increased. And in vivo experiments, the levels of TLR4 and MyD88 in the liver of model group animals also showed a significant increase. To investigate whether this pathway is the mechanism by which ACY-1215 protects NAFLD, we further tested the expression levels of related proteins. In both in vitro and in vivo experiments, ACY-1215 significantly reduced the expression levels of CD14, TLR4, and MyD88, while in the model group, the expression levels of these proteins were significantly increased. Meanwhile, ACY-1215 can reduce the phosphorylation forms of MAPK p38, MAPK p42/44, and NF κ B p65, indicating that the activation of the MAPK/NF κ B signaling pathway is inhibited. Therefore, we believe that the CD14/TLR4/MyD88/MAPK/NF κ B signaling pathway is indeed involved in the protective effect of ACY-1215 on NAFLD.

Gut microbiota refers to the sum of all microorganisms naturally existing in the gastrointestinal tract. In recent decades, people have found that gut microbiota has a considerable impact on the metabolism of the body and the occurrence of diseases. LPS is the main component of the cell wall of Gram-negative bacteria and a strong inflammatory activator, belonging to the pathogen-associated molecular patterns (PAMPs). Gut microbiota, intestinal barrier, and LPS are closely related to the pathogenesis and development of NAFLD. Under physiological conditions, because there is an intestinal barrier in the body's intestinal tract, a small amount of LPS produced by gut microbiota is difficult to enter the circulation through the intestinal tract [31]. In animal models of NAFLD induced by different diets such as HFD, fructose-rich diets, or diets lacking methionine and choline, it was found that the concentration of LPS in the circulation was higher than normal [32–35]. The stimulation of adding LPS under a normal diet will also lead to an increase in fasting blood sugar, weight gain, insulin resistance, liver steatosis, liver TG content, and inflammatory factor secretion in experimental animals [35]. Adding LPS stimulation to the NAFLD animal model will further exacerbate the release of inflammatory factors and promote more severe liver damage [36,37]. Nakanishi and colleagues reported that LPS can induce more severe insulin resistance in NAFLD model mice, and upregulate adipogenic genes to exacerbate liver steatosis, promoting inflammatory cell infiltration into the liver [38]. Some studies have reported that long-term intake of a high-calorie diet can induce metabolic disorders and intestinal ecological disorders [39,40]. The intestinal barrier of NAFLD patients is usually damaged, and LPS produced by bacteria in the intestine is more likely to enter the circulation through the intestinal barrier [41]. Multiple studies have reported an increase in LPS concentration in the blood of NAFLD patients [42–44]. Nier et al. reported that even in adolescent patients with early NAFLD, plasma LPS levels have increased, suggesting that intestinal barrier dysfunction may have already appeared in the early stages of NAFLD [42]. Any trace amount of LPS present in the circulation can activate inflammatory responses through the CD14/TLR4 signaling [45]. The activation of inflammation by LPS is mainly mediated by the CD14 and TLRs signaling pathways. After reaching the liver, LPS first binds to LBP to form the LBP-LPS complex [37,45]. The LBP-LPS complex interacts with CD14 on the cell membrane surface and is transferred to the TLR4-MD2 complex, activating the intracellular domain Toll/IL-IR of TLR4 [37,45]. Once LPS binds to the TLR4-CD14-MD2 complex, TLR4 undergoes oligomerization and conformational changes in the extracellular structure, causing dimerization of the Toll/IL-IR domain within the cytoplasm, allowing downstream adapters to recruit through interactions with the Toll/IL-IR domain to trigger downstream signals [37,45]. There are two downstream signaling pathways, namely the MYD88 dependent pathway and the MYD88 independent pathway. In liver cells, the latter has a slower signal transmission and delayed activation of subsequent inflammatory responses [45]. Under the stimulation of ligands, MYD88 will recruit and activate IRAK4, which can activate TAK1 in the MAPK family [37,45]. TAK1 will phosphorylate the IKK β subunit in the NF κ B signaling pathway through the ubiquitin chain, causing degradation of the IKK β subunit and releasing free NF κ B complexes (p50/p65) [37,45]. At the same time, the IKK complex will phosphorylate the NF κ B inhibitory protein IKBA, allowing the NF κ B complex to translocate into the nucleus and initiate the transcription of pro-inflammatory genes including IL-1 β , TL-6, TL-18, and TNF α [37,45]. The excessive activation of the TLR4 signaling pathway can lead to the worsening of liver inflammation, manifested as increased infiltration of inflammatory factors and increased chemotaxis of immune cells, and even lead to liver fibrosis, thereby promoting the occurrence of cirrhosis [46–48]. Many studies have also reported that knocking out or knocking down CD14 or TLR4 can make experimental animals gain resistance to NAFLD [32,34,49,50]. In addition, activation of the MAPK/NF κ B signaling pathway through different pathways can induce inflammatory responses and exacerbate NAFLD, and much evidence has been obtained [51–54]. The use of different drugs to inhibit the activation of MAPK/NF κ B signaling pathways through different pathways can improve NAFLD and slow down its development [51,55,56]. Therefore, from the perspective of inflammatory activation, the MAPK/NF κ B signaling pathway seems to be the core of the influence of different pathways. These reports are consistent with our experimental results and suggest that ACY-1215 may have a

blocking effect on the development of NAFLD in the early stages. Reducing the inflammatory response caused by LPS and suppressing the inflammatory factor storm in the liver may be an important step in preventing the development of NAFL towards NASH.

This study is the first to apply ACY-1215 to the experimental model of NAFLD and verifies the role of ACY-1215. It is proposed that CD14 may be the target of the protective effect of ACY-1215 on NAFLD. Through CD14, we have linked intestinal microbiota disorders with the onset of NAFLD and proposed a new strategy to intervene in the progression of NAFLD. There are also some limitations in this study. Although we observed weight loss in experimental animals after treatment with ACY-1215, we cannot determine whether the off-target toxicity of ACY-1215 is involved. We have not yet elucidated the impact of up-regulation or down-regulation of CD14 on the effects of HDAC6 and ACY-1215 or the development of NAFLD, and how HDAC6 affects CD14 expression. Therefore, the next stage of research will further explore the relationship between HDAC6 and CD14, as well as the role of CD14 in the pathogenesis and development of NAFLD, by constructing gene-manipulated cell and animal models.

In conclusion, this study verified the protective effect of ACY-1215 on NAFLD and preliminarily explored the mechanism of ACY-1215 through TMT relative quantitative proteomics. ACY-1215 can inhibit the activation of the CD14/TLR4/MyD88/MAPK/NFκB signaling pathway and has a protective effect on NAFLD cells and animal models.

Lay summary

This research finds a drug that may be beneficial for non-alcoholic fatty liver disease, which may act by inhibiting the activation of inflammatory responses.

Ethics approval statement

Animal ethics has been approved by the Experimental Animal Ethics Committee of Xiangya Medical College (CSU-2022-0033).

Funding statement

The study was supported by Health Research Project of Hunan Provincial Health Commission (grant number:202103030980) and Natural Science Foundation of Hunan Province (no. 2022JJ30837).

Data availability statement

Data will be made available on request.

CRediT authorship contribution statement

Shifeng Fu: Writing – review & editing, Writing – original draft, Methodology, Investigation, Formal analysis, Data curation, Conceptualization. **Mengmeng Xu:** Writing – review & editing, Writing – original draft, Methodology, Investigation, Formal analysis, Data curation. **Jianglei Li:** Writing – review & editing, Writing – original draft, Methodology, Investigation, Formal analysis, Data curation. **Meihong Yu:** Writing – review & editing, Writing – original draft, Methodology, Investigation, Formal analysis, Data curation, Conceptualization. **Siyi Wang:** Writing – review & editing, Writing – original draft, Validation, Resources, Methodology, Investigation. **Liu Han:** Writing – review & editing, Writing – original draft, Methodology, Investigation, Formal analysis, Data curation. **Rong Li:** Writing – review & editing, Writing – original draft, Validation, Formal analysis, Conceptualization. **Feihong Deng:** Writing – review & editing, Writing – original draft, Validation, Resources, Formal analysis, Conceptualization. **Hailing Peng:** Writing – review & editing, Writing – original draft, Methodology, Formal analysis, Data curation. **Deliang Liu:** Writing – review & editing, Writing – original draft, Supervision, Resources, Project administration, Funding acquisition, Formal analysis, Data curation, Conceptualization. **Yuyong Tan:** Writing – review & editing, Writing – original draft, Supervision, Resources, Project administration, Methodology, Funding acquisition, Formal analysis, Data curation, Conceptualization.

Declaration of competing interest

The authors declare the following financial interests/personal relationships which may be considered as potential competing interests: Tan Yuyong reports financial support was provided by Hunan Province Health Commission. If there are other authors, they declare that they have no known competing financial interests or personal relationships that could have appeared to influence the work reported in this paper.

Acknowledgments

Thanks to Zhongke New Life (Zhejiang) Biotechnology Co., Ltd. For the help of the proteomics part of this study.

References

- [1] Z.M. Younossi, et al., Global epidemiology of nonalcoholic fatty liver disease-Meta-analytic assessment of prevalence, incidence, and outcomes, *Hepatology* 64 (1) (2016) 73–84.
- [2] M. Sayiner, et al., Epidemiology of nonalcoholic fatty liver disease and nonalcoholic steatohepatitis in the United States and the rest of the world, *Clin. Liver Dis.* 20 (2) (2016) 205–214.
- [3] F. Zhou, et al., Unexpected rapid increase in the burden of NAFLD in China from 2008 to 2018: a systematic review and meta-analysis, *Hepatology* 70 (4) (2019) 1119–1133.
- [4] H. Tilg, A.R. Moschen, Evolution of inflammation in nonalcoholic fatty liver disease: the multiple parallel hits hypothesis, *Hepatology* 52 (5) (2010) 1836–1846.
- [5] C.D. Byrne, G. Targher, NAFLD: a multisystem disease, *J. Hepatol.* 62 (1 Suppl) (2015) S47–S64.
- [6] J. Zhou, et al., Epidemiological features of NAFLD from 1999 to 2018 in China, *Hepatology* 71 (5) (2020) 1851–1864.
- [7] A. Inoue, D. Fujimoto, Enzymatic deacetylation of histone, *Biochem. Biophys. Res. Commun.* 36 (1) (1969) 146–150.
- [8] E. Seto, M. Yoshida, Erasers of histone acetylation: the histone deacetylase enzymes, *Cold Spring Harb Perspect Biol* 6 (4) (2014) a018713.
- [9] S. Fu, et al., Role of histone deacetylase on nonalcoholic fatty liver disease, *Expet Rev. Gastroenterol. Hepatol.* 15 (4) (2021) 353–361.
- [10] Y. Liu, et al., Insulin/Sna11 axis ameliorates fatty liver disease by epigenetically suppressing lipogenesis, *Nat. Commun.* 9 (1) (2018) 2751.
- [11] H. Zhang, et al., Targeting epigenetically maladapted vascular niche alleviates liver fibrosis in nonalcoholic steatohepatitis, *Sci. Transl. Med.* 13 (614) (2021) eabd1206.
- [12] N. Liang, et al., The nuclear receptor-Co-repressor complex in control of liver metabolism and disease, *Front. Endocrinol.* 10 (2019) 411.
- [13] N. Liang, et al., Hepatocyte-specific loss of GPS2 in mice reduces non-alcoholic steatohepatitis via activation of PPAR α , *Nat. Commun.* 10 (1) (2019) 1684.
- [14] C.Y. Zhang, et al., COX-2/sEH dual inhibitor alleviates hepatocyte senescence in NAFLD mice by restoring autophagy through Sirt1/PI3K/AKT/mTOR, *Int. J. Mol. Sci.* 23 (15) (2022).
- [15] Y. Liu, et al., Salvia-Nelumbinis naturalis improves lipid metabolism of NAFLD by regulating the SIRT1/AMPK signaling pathway, *BMC Complement Med Ther* 22 (1) (2022) 213.
- [16] X.D. Yang, et al., Esculin protects against methionine choline-deficient diet-induced non-alcoholic steatohepatitis by regulating the Sirt1/NF- κ B p65 pathway, *Pharm. Biol.* 59 (1) (2021) 922–932.
- [17] H. Leal, et al., SIRT2 deficiency exacerbates hepatic steatosis via a putative role of the ER stress pathway, *Int. J. Mol. Sci.* 23 (12) (2022).
- [18] H. Ren, et al., Sirtuin 2 prevents liver steatosis and metabolic disorders by deacetylation of hepatocyte nuclear factor 4 α , *Hepatology* 74 (2) (2021) 723–740.
- [19] L. Xie, et al., CD38 deficiency protects mice from high fat diet-induced nonalcoholic fatty liver disease through activating NAD(+)/Sirtuins signaling pathways-mediated inhibition of lipid accumulation and oxidative stress in hepatocytes, *Int. J. Biol. Sci.* 17 (15) (2021) 4305–4315.
- [20] R.A. Bagchi, et al., HDAC11 suppresses the thermogenic program of adipose tissue via BRD2, *JCI Insight* 3 (15) (2018).
- [21] L. Sun, et al., Programming and regulation of metabolic homeostasis by HDAC11, *EBioMedicine* 33 (2018) 157–168.
- [22] L. Santo, et al., Preclinical activity, pharmacodynamic, and pharmacokinetic properties of a selective HDAC6 inhibitor, ACY-1215, in combination with bortezomib in multiple myeloma, *Blood* 119 (11) (2012) 2579–2589.
- [23] B. Deskin, et al., Inhibition of HDAC6 attenuates tumor growth of non-small cell lung cancer, *Transl Oncol* 13 (2) (2020) 135–145.
- [24] T. Oba, et al., HDAC6 inhibition enhances the anti-tumor effect of eribulin through tubulin acetylation in triple-negative breast cancer cells, *Breast Cancer Res. Treat.* 186 (1) (2021) 37–51.
- [25] Y. Tan, et al., Histone deacetylase 6 selective inhibitor ACY1215 inhibits cell proliferation and enhances the chemotherapeutic effect of 5-fluorouracil in HCT116 cells, *Ann. Transl. Med.* 7 (1) (2019) 2.
- [26] C. Cheng, et al., ACY-1215 exhibits anti-inflammatory and chondroprotective effects in human osteoarthritis chondrocytes via inhibition of STAT3 and NF- κ B signaling pathways, *Biomed. Pharmacother.* 109 (2019) 2464–2471.
- [27] Q. Chen, et al., Histone deacetylase 6 inhibitor ACY1215 offers a protective effect through the autophagy pathway in acute liver failure, *Life Sci.* 238 (2019) 116976.
- [28] W.B. Zhang, et al., Histone deacetylase 6 inhibitor ACY-1215 protects against experimental acute liver failure by regulating the TLR4-MAPK/NF- κ B pathway, *Biomed. Pharmacother.* 97 (2018) 818–824.
- [29] Y. Wang, et al., Histone deacetylase 6 regulates the activation of M1 macrophages by the glycolytic pathway during acute liver failure, *J. Inflamm. Res.* 14 (2021) 1473–1485.
- [30] D.T. Vogl, et al., Ricolinostat, the first selective histone deacetylase 6 inhibitor, in combination with bortezomib and dexamethasone for relapsed or refractory multiple myeloma, *Clin. Cancer Res.* 23 (13) (2017) 3307–3315.
- [31] Y. Mimura, et al., Role of hepatocytes in direct clearance of lipopolysaccharide in rats, *Gastroenterology* 109 (6) (1995) 1969–1976.
- [32] C.A. Rivera, et al., Toll-like receptor-4 signaling and Kupffer cells play pivotal roles in the pathogenesis of non-alcoholic steatohepatitis, *J. Hepatol.* 47 (4) (2007) 571–579.
- [33] Y. Kodama, et al., c-Jun N-terminal kinase-1 from hematopoietic cells mediates progression from hepatic steatosis to steatohepatitis and fibrosis in mice, *Gastroenterology* 137 (4) (2009) 1467–1477.e5.
- [34] T. Csak, et al., Deficiency in myeloid differentiation factor-2 and toll-like receptor 4 expression attenuates nonalcoholic steatohepatitis and fibrosis in mice, *Am. J. Physiol. Gastrointest. Liver Physiol.* 300 (3) (2011) G433–G441.
- [35] P.D. Cani, et al., Metabolic endotoxemia initiates obesity and insulin resistance, *Diabetes* 56 (7) (2007) 1761–1772.
- [36] K. Imajo, et al., Hyperresponsivity to low-dose endotoxin during progression to nonalcoholic steatohepatitis is regulated by leptin-mediated signaling, *Cell Metabol.* 16 (1) (2012) 44–54.
- [37] H. Kudo, et al., Lipopolysaccharide triggered TNF-alpha-induced hepatocyte apoptosis in a murine non-alcoholic steatohepatitis model, *J. Hepatol.* 51 (1) (2009) 168–175.
- [38] K. Nakanishi, et al., Exogenous administration of low-dose lipopolysaccharide potentiates liver fibrosis in a choline-deficient l-amino-acid-defined diet-induced murine steatohepatitis model, *Int. J. Mol. Sci.* 20 (11) (2019).
- [39] X. Guo, et al., High fat diet alters gut microbiota and the expression of paneth cell-antimicrobial peptides preceding changes of circulating inflammatory cytokines, *Mediat. Inflamm.* 2017 (2017) 9474896.
- [40] J.M. Li, et al., Dietary fructose-induced gut dysbiosis promotes mouse hippocampal neuroinflammation: a benefit of short-chain fatty acids, *Microbiome* 7 (1) (2019) 98.
- [41] K. Miura, H. Ohnishi, Role of gut microbiota and Toll-like receptors in nonalcoholic fatty liver disease, *World J. Gastroenterol.* 20 (23) (2014) 7381–7391.
- [42] A. Nier, et al., Markers of intestinal permeability are already altered in early stages of non-alcoholic fatty liver disease: studies in children, *PLoS One* 12 (9) (2017) e0183282.
- [43] A.L. Harte, et al., Elevated endotoxin levels in non-alcoholic fatty liver disease, *J. Inflamm.* 7 (2010) 15.
- [44] D. Satoh, et al., CD14 upregulation as a distinct feature of non-alcoholic fatty liver disease after pancreatoduodenectomy, *World J. Hepatol.* 5 (4) (2013) 189–195.
- [45] S. Mohammad, C. Thiemermann, Role of metabolic endotoxemia in systemic inflammation and potential interventions, *Front. Immunol.* 11 (2020) 594150.
- [46] S. Khanmohammadi, M.S. Kuchay, Toll-like receptors and metabolic (dysfunction)-associated fatty liver disease, *Pharmacol. Res.* 185 (2022) 106507.
- [47] Y. Shirai, et al., Cross talk between toll-like receptor-4 signaling and angiotensin-II in liver fibrosis development in the rat model of non-alcoholic steatohepatitis, *J. Gastroenterol. Hepatol.* 28 (4) (2013) 723–730.
- [48] J. Li, et al., Resolvin D1 mitigates non-alcoholic steatohepatitis by suppressing the TLR4-MyD88-mediated NF- κ B and MAPK pathways and activating the Nrf2 pathway in mice, *Int. Immunopharm.* 88 (2020) 106961.

- [49] M. Poggi, et al., C3H/HeJ mice carrying a toll-like receptor 4 mutation are protected against the development of insulin resistance in white adipose tissue in response to a high-fat diet, *Diabetologia* 50 (6) (2007) 1267–1276.
- [50] P.D. Cani, et al., Changes in gut microbiota control metabolic endotoxemia-induced inflammation in high-fat diet-induced obesity and diabetes in mice, *Diabetes* 57 (6) (2008) 1470–1481.
- [51] X. Zhang, et al., Macrophage p38 α promotes nutritional steatohepatitis through M1 polarization, *J. Hepatol.* 71 (1) (2019) 163–174.
- [52] Z. Hu, et al., Role of Asxl2 in non-alcoholic steatohepatitis-related hepatocellular carcinoma developed from diabetes, *Int. J. Mol. Med.* 47 (1) (2021) 101–112.
- [53] Z.M. Younossi, et al., An exploratory study examining how nano-liquid chromatography-mass spectrometry and phosphoproteomics can differentiate patients with advanced fibrosis and higher percentage collagen in non-alcoholic fatty liver disease, *BMC Med.* 16 (1) (2018) 170.
- [54] J. Ye, et al., Integrated multichip analysis identifies potential key genes in the pathogenesis of nonalcoholic steatohepatitis, *Front. Endocrinol.* 11 (2020) 601745.
- [55] S. Alshehade, et al., The role of protein kinases as key drivers of metabolic dysfunction-associated fatty liver disease progression: new insights and future directions, *Life Sci.* 305 (2022) 120732.
- [56] S.H. Ibrahim, et al., Nonalcoholic steatohepatitis promoting kinases, *Semin. Liver Dis.* 40 (4) (2020) 346–357.